Information Sciences Letters
An International Journal

http://dx.doi.org/10.18576/isl/121016

Appropriate and Optimal Classifier for Beef Quality Discrimination by A Low-Cost Optical Apparatus

Said E. Abdallah[1], Wael M. Elmessery[1], Waleed Z. Hassan[2], Nora S. Al-Sattary[1], Amr A. Abohany[3] and Ahmed Elashry[3,]*

[1]Department of Agricultural Engineering, Faculty of Agriculture, Kafrelsheikh University, Kafr Elsheikh 33516, Egypt
[2]Department of Food Technology, Faculty of Agriculture, Kafrelsheikh University, Kafr Elsheikh 33516, Egypt
[3]Department of Information Systems, Faculty of Computers and Information, Kafrelsheikh University, Kafr Elsheikh 33516, Egypt

Received: 23 Jul. 2023, Revised: 29 Aug. 2023, Accepted: 2 Sep. 2023
Published online: 1 Oct. 2023.

Abstract: In this paper, we present an optimal classifier for beef quality discrimination by a low-cost optical apparatus. Detecting beef spoilage in beef factories is a sophisticated process because beef spoilage is a mixture of physical and chemical changes. A low-cost Light-Dependent Resistor (LDR), and a light source were used to collect reflection spectra during the analysis of beef. The LabVIEW platform was programmed to acquire the obtained data from the microcontroller (Arduino) to predict beef quality. For the beef quality discrimination process, un-supervising machine learning called Principal Components Analysis (PCA) was used, and the score plot percentage was of the first (F1) and second (F2) dimensions of the most variation for forty samples were of 93.98% and 3.38% respectively. Supervised Machine Learning (SML) (Support Vector Machine (SVM) and Linear Discriminant Analysis (LDA)) were used also to compare with other models of un-supervised machine learning. Optimum classifier was achieved by the classification algorithm of SVM that can represent 95.75% of the whole data.

Keywords: Non-destructive beef quality analysis, machine learning models, classification models, Support Vector Machine.

1 Introduction

The beef industry has recently become widespread, that represented in the storage processes by [1, 2], freezing [3-10] and drying [7, 11-13]. The beef quality problems in the production lines are in color, smell and texture, so beef industry professionals are concerned to obtain the highest quality when they reach to consumer. The old traditional methods of detecting beef spoilage have become inappropriate and inaccurate. In recent times, the spread of modern non-destructive technologies in food industry has increased, such as computer vision [14-20] , spectroscopy [21-23], electronic nose [24-27], imaging [8, 9, 11, 28-40] and hyperspectral [30]. But despite these previous measures are accurate and non-destructive techniques, they are very expensive. In recent times, technological intervention has increased, which includes artificial intelligence, in many food industries, as the machine has become a substitute for humans in many tasks such as classification, object recognition and computer vision [41, 42] Artificial intelligence includes two main concepts, the neural network and deep learning, as thanks to the development in artificial intelligence, the machine has become able to learn by simulating human thinking and analyzing a huge amount of data [43]. The effect of using artificial intelligence and image processing on many industries, including the food industry, such as identifying food quality and classifying it [44-46]. Machine learning is divided into two types: first, supervised machine learning, which contains inputs through which outputs is predicted. Secondly, learning without supervision is used when data is not disaggregated for training used to describe its hidden structures from unclassified data [47-49]. Support Vector Machine (SVM) system is a type of artificial intelligence science; it is a method of learning under supervision. SVM is used for regression analysis and classification, such as the classification of image faces and hand gesture recognition [50]. The idea of SVM is based on classification of the data with an imaginary line and that there is a barrier separating the points and each other. This barrier is called optimal hyper-plane [51-53]. The nearest distance between two different points is called the maximum margin, where the location and the boundary of the barrier are determined by accurate calculations, and the line that represents the end of each part is called the support vector [54]. The speed of classification by SVM is large and the separator type is non-linear due to the presence of non-overlapping distances. More than one type of function can be used such as sigmoid and tanh function [55]. There are several types of SVM such as kernel, power, and redial basic function. The kernel similarity function is used in prediction to compare

*Corresponding author e-mail: ahmed_elashry@fci.kfs.edu.eg

values given with the existing values [56]. There are two types of Kernels, such as Linear Kernels and Gaussian Kernel. The approach or distance of specific point from rest of points in the system is calculated through the similarity function called Gaussian Kernel [57]. The idea of Linear Discriminant Analysis (LDA) is based on Fisher's distinction, which is a statistical method that performs classification process by finding a linear group or combination of features to distinguish among two or more classes of existing data [58]. The analysis of LDA depends on the Analysis of Variance (ANOVA) and regression analysis, by finding the dependent variable as a linear group of a set of extra characteristics or data. However, the analysis of variance depends on independent variables and dependent variables while LDA depends on independent variables and a class dependent variable such as, the class name [59-61]. Logistic regression and regression with unit probability are more similar to LDA than to analysis of variance, as they share in classification of the dependent variable by values of the independent variable. The two methods of logistic regression and regression are more common, as it is not acceptable to assume that the independent variables follow a normal distribution, and it is a basic assumption for the method of analysis of linear discrimination [62, 63]. LDA is also closely related to the principal component analysis and factor analysis as they search for linear structures of variables that better illustrate the data [64]. LDA tries to distinguish among data categories by knowing the differences between sets of data and the correspondences, so it ultimately classifies the data [65, 66]. LDA also differs from the factor analysis in that it is not a correlation method, as it is necessary to separate the independent and dependent variables [38]. Principal Components Analysis (PCA) is a method for analyzing data by reducing dimensions [67, 68]. PCA is a type of education the machine without supervision means it is a learning that results from having data without its correct readings [69]. One of the most common types of learning without supervision is cluster analysis [70, 71]. The analysis of PCA is an arithmetic operation that aims to reduce points from the best fit line by reducing data, and as a result of this, the distance between data increases, the variance increases and data can be classified faster and better. The condition of data reduction is that the data are related to each other. In the present study, the classification process was performed depending on frequencies of the colors resulting from Red, Green, and Blue (RGB) color sensor and reflection of spectra resulting from the interaction between light and the samples. In order to reduce and represent data dimensions, Principal Components Analysis was used as a model for unsupervised learning. SVM and LDA were used as a model for supervised machine learning. Therefore, this investigation is tried to find an optimum machine learning classifier suitable for low-cost optical device to measure the quality of beef without destruction.

2 Materials and Methods

2.1 Reference Measurement

The beef piece was brought four hours after the slaughtering process, and then it was divided into forty samples with a thickness of 0.5mm. The samples were manually divided into two groups. The calibration and validation groups consist of twenty-six samples and sixteenth samples, respectively. After that, the samples were placed in plastic bags sterilized in the refrigerator at a temperature of 4°C for the physical and chemical analysis process over ten days. The protein content of samples was measured using the Kjeldahl method at the laboratories of Food Technology Department, Faculty of Agriculture, Kafr elsheikh University, Egypt in January 2020. The mean of protein value and standard deviation of beef samples was 25.25 ± 1.87mg protein/g beef.

3 Low-cost Beef Spoilage Sensing Unit

3.1 Data Acquisition System

Figure 1 shows data acquisition system of beef samples. The optical characteristics of each beef sample were measured by RGB (TCS3200) color sensor and Light-Dependent Resistor (LDR) over storage days. Light source (solar lamp) of 5W.

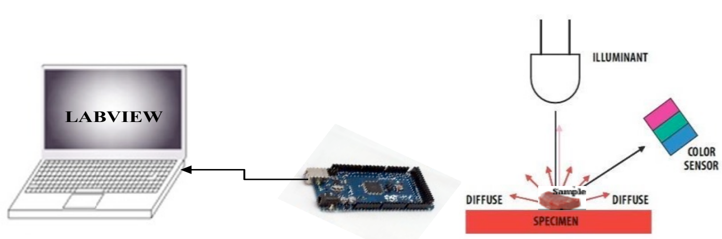

Fig. 1: Computer vision and spectrum system

The specifications of the 12mm LDR were of light resistance of 5-100KΩ and dark resistance of 1-8MΩ. Figure 2 shows the connection diagram of the LDR to the Arduino board, where the signal terminal of the sensor is connected to the analog pin of A0 of the Arduino.

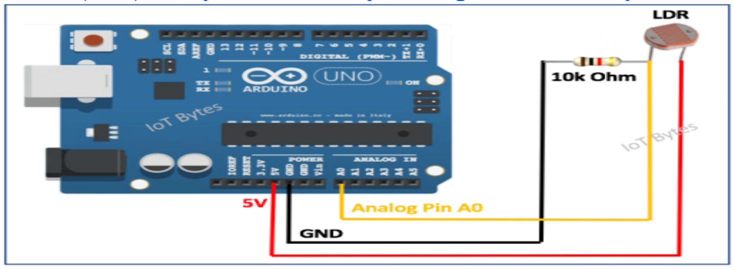

Fig. 2: Drawing of LDR hardware system for measuring the light of density

3.2 Beef Quality Visualization by LabVIEW Platform

LabVIEW program platform was used to visualize the classification results obtained by the developed classifier. Figure 3 shows the two panels of the program; (1) Block Diagram (back) panel, that provides the developer with a graphical code for programming, and (2) Front Panel which affords and represents the acquired data, and discrimination results of beef quality (Healthy or Rancid).

3.3 Data Receiving and Analyzing System

Once the microcontroller of Arduino has acquired the data from the sensors of RGB and LDR, then the microcontroller can transmit these data to the personal computer prepared with LabVIEW, 2013 software. The interface of LabVIEW program consists of Block Diagram, Front Panel, and connector pane. The Front Panel includes controls and indicators. Block Diagram is containing the graphical source code. Hence any object on the front panel appears as a terminal on the Block Diagram [72]. Virtual Instrument Software Architecture (VISA) resource name control was used to specify the resources to which a (VISA) session can be opened and to maintain the session and class. The data can be transferred through USB/Serial. The data transfer rate (baud rate) was 115 200baud/second. Reflection spectra values were sent by Arduino interface to the software constructed by LabVIEW package and control software programming platform.

3.4 Support Vector Machine

Linear support vector machine was used to classify quality of beef (healthy and rancid). Hyperplane and hard margins were calculated through the following equation [73, 74]:

$$\vec{w} = \Sigma_i \; y_i \, \alpha_i \, \vec{x_i} \tag{1}$$

$$\vec{w}.\vec{x_i} - b = 0, \tag{2}$$

$$\vec{w}.\vec{x_i} - b \geq 1 \;\; \text{if} \;\; y_i = 1 \tag{3}$$

or

$$\vec{w}.\vec{x_i} - b \leq -1 \;\; \text{if} \;\; y_i = -1 \tag{4}$$

Where $\vec{w}$ is the normal vector, $\vec{x_i}$ is dimensional real vector, where y_i are either 1 or −1, each indicating the class to which the point $\vec{x_i}$ belongs, b is bias, and α_i is parameters alpha.

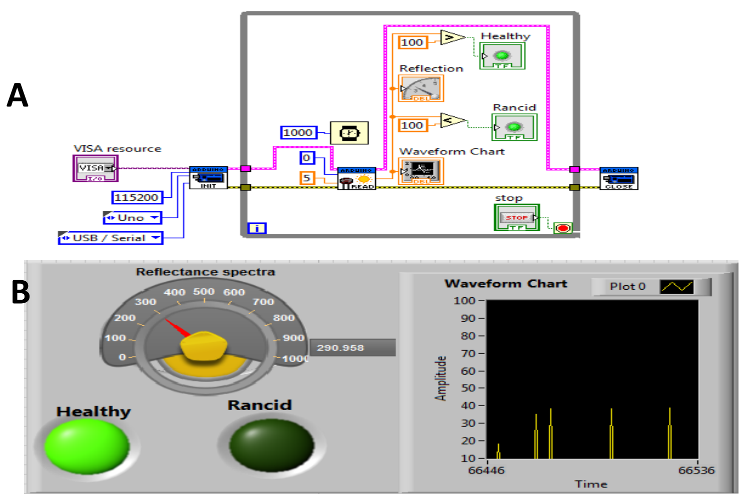

Fig. 3: Beef quality visualization by LabVIEW (a) programing panel block diagram, (**BD)** and (b) Front panel \ data representation panel, **(FP)**

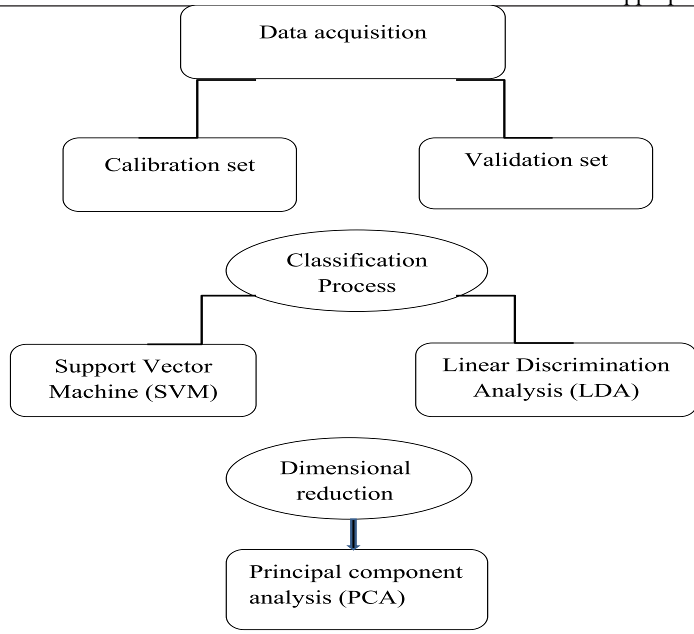

Fig. 4: Acquired data processing flowchart for optimum classifier determination

3.5 Mathematical Approach of LDA

Linear Discrimination Analysis works successfully when the independent variables measures are related to categorical dependent variables. The linear discrimination analysis method is considered the best in the classification process when dealing with categorical independent variables. Two natural distributions with an arithmetic mean and a coefficient of variation represent the classes of rancid and healthy beef. According to this hypothesis, the best solution for Bayes is to classify points for the first or second category [75]. If the logarithm of the likelihood ratio is greater than the intensity of the threshold (Equation 5), so that can be classified as out:

$$(\vec{x}-\vec{\mu_0})^T \textstyle\sum_0^{-1}(\vec{x}-\vec{\mu_0})+\ln|\Sigma_0|-(\vec{x}-\vec{\mu_1})^T \textstyle\sum_1^{-1}(\vec{x}-\vec{\mu_1}) \ln|\Sigma_1| > T \quad (5)$$

LDA assumes simplicity equal to variance (for example that the coefficients of variants of the two classes are identical, therefore ($\Sigma_1 = \Sigma_0 = \Sigma$), and that the coefficients of variance have a complete degree. In this case, several algebraic amounts can be omitted from the equations:

$$\vec{x}^T \textstyle\sum_0^{-1} \vec{x}=\vec{x}^T \textstyle\sum_1^{-1} \vec{x} \quad (6)$$

For some threshold constant c, where:

$$\vec{w}=\Sigma^{-1}(\vec{\mu_1}-\vec{\mu_0}) \quad (7)$$

$$C=\frac{1}{2}(T-\vec{\mu_0}^T \textstyle\sum_0^{-1}\vec{\mu_0}+\vec{\mu_1}^T \textstyle\sum_1^{-1}\vec{\mu_1}) \quad (8)$$

$$\vec{w}.\vec{x} > c \quad (9)$$

Where μ_1, μ_0 are mean; Σ_1, Σ_0 are covariances; T is thresholding; $\vec{x}$ is observation set; $\vec{w}$ is the normal vector to the discriminant hyperplane; and c is border line.

3.6 Principal Components Analysis

Eigenvector is a matrix column that expresses contrast or correlation to determine the degree of PCA through the following equation [76].

$$R = V D V' \quad (10)$$

Where R is correlation matrix, V' eigenvector matrix, and D is diagonal matrix of eigenvalues. Eigenvalues represent the variables in the correlation or contrast matrix and are calculated from the following equation:

$$Z = V Y \quad (11)$$

Where z is matrix of principal components scores ($n \times m$), Y is standardized data matrix ($n \times p$) used with the correlation matrix method, V is matrix of eigenvectors ($p \times m$), and n, p, and m are number of row and column of the matrix. The variance values for the variables are calculated by the following equation:

$$\frac{\lambda_k}{\lambda_1+\lambda_2+\cdots+\lambda_b} \quad (12)$$

Where λ_k the eigenvalue, and b is the number of variables. The Mahalanobis measures the distance between the points of the variables to the central mean by the following equation:

$$Y_i=\sqrt{((Y_i-\bar{Y})S^{-1}(Y_i-\bar{Y}))} \quad (13)$$

Where Y_i data value vector at row i, and $\bar{Y}$ is mean vector. S-1 inverse of the covariance matrix, p is the number of variables, n is the number of Non-missing rows.

4 Results and Discussion

4.1 Classification Process with SVM

Linear Kernel Support Vector Machine (SVM) model was used to classify data samples. The samples were divided into calibration set and validation set. SVM was built upon frequencies data acquired by the RGB color sensor and reflection of spectra during storage days. Table 1 indicates the classifier characteristics which can classify rancid and healthy samples of beef (rancid was the positive class). There were twenty four classifiers out of which twelve support vectors have been identified; the bias was of -1.395.

Table 1: Classifier for classes (rancid and healthy) beef

Positive class	Rancid
Number of observations in the training set	24.000
Bias	-1.395
Number of support vectors	12.000

The whole list of the twelve support vectors associated with their alpha coefficient and the output class values (positive or negative) was listed in Table 2. Composed with the bias value of the Table 1, this information is sufficient to fully describe the optimum classifier. Table 3 indicates the total classification percentage for the calibration set was of 95.83% and the validation set was of 93.75%.

Table 2: List of support vector machine

quality	alpha	Reflection	Blue	Green	Red
-1	0.324	0.520	0.375	0.363	0.582
-1	1.000	0.391	0.462	0.323	0.549
-1	1.000	0.262	0.278	0.254	0.220
-1	1.000	0.293	0.280	0.209	0.412
-1	1.000	0.309	0.320	0.266	0.478
-1	1.000	0.352	0.236	0.182	0.357
1	0.324	0.066	0.000	0.127	0.115
1	1.000	0.063	0.077	0.005	0.154
1	1.000	0.109	0.112	0.072	0.060
1	1.000	0.121	0.139	0.100	0.093
1	1.000	0.098	0.084	0.047	0.170
1	1.000	0.070	0.052	0.002	0.198

Table 3: Confusion matrix for calibration and validation sets

	Calibration set				Validation set			
From/to	rancid	healthy	Total	% correct	Rancid	healthy	Total	% correct
rancid	9	0	9	100.00	1	0	1	100.00
healthy	1	14	15	93.33	1	14	15	93.33
Total	10	14	24	95.83	2	14	16	93.75

4.2 Classifier Determination by LDA Method

4.2.1 Classes' Relations and Locations

Table 4 illustrates the mean among classes of the samples. Table 5 indicates the sum of weights, the previous probabilities and the logarithms of the determinants for each category that were selected and used in the calculation of proposed probabilities.

Table 4: Means by class

Class \ Variable	Reflection	Blue	Green	Red
rancid (μ_0)	97.667	81.500	121.833	166.333
healthy (μ_1)	229.611	250.944	318.389	256.833

Table 5: Sum of weights, prior probabilities and logarithms of determinants for each class

Class	Sum of weights	Prior probabilities	Log (Determinant)
rancid	6.000	0.250	17.445
healthy	18.000	0.750	27.579

Table 6 illustrates Multicolinearity statistics: Displays multiple linearity statistics: This table identifies the variable (reflection, red, green, and blue frequencies of the color) responsible for the Multicolinearity among variables. When there is a similarity between two variables, the variable causing linear multiplicity will be eliminated. The presence of linear multiplicity is determined by the tolerance factor (equal to 1-R^2) and the Variance Inflation Factor (VIF). As VIF is greater than 10, there is a high probability of multicolinearity.

Table 6: Multicolinearity statistics

Statistic	Reflection	Blue	Green	Red
Tolerance	0.049	0.048	0.051	0.101
VIF	20.432	20.853	19.496	9.870

4.3 Covariance Matrices of Inter and Intra Classes

Table 7 demonstrates covariance matrices: Covariance is a measure of the extent of difference or dispersion between two variables, and it is a matrix consisting of two elements X and Y. The covariance may be positive or negative covariance, and when the two variables are equal, the variance becomes covariance. The covariance matrix may be between classes (inter-class) or within each layer of a single class (intra-class).

Table 7: Total covariance matrix

	Reflection	Blue	Green	Red
Reflection	7046.245	8914.359	9689.402	3833.299
Blue	8914.359	12046.688	12624.848	5118.047
Green	9689.402	12624.848	14443.761	5656.120
Red	3833.299	5118.047	5656.120	2502.520

4.4 Intra-Classes Covariance Matrix Un-equality Test

The equality of the covariance matrices within a layer (Intra-classes) is determined by the Box test. There are two tests, one based on the Chi-square distribution, and the other on the Fisher distribution. In the box test (asymptotic approximation of Chi square), since the resulting P-value is less than the level of significance alpha = 0.05, the null hypothesis H0 that assumes the mean vectors of the two classes are equal, must be rejected, and the alternative can be acceptable to the hypothesis Ha that assumes that one of the two classes is different from the other class. The same results are achieved by the Box test (Fisher asymptotic F approximation), P-value is less than alpha significance level = 0.05, as depicted in Table 8.

Table 8: Box test (Chi-square asymptotic approximation) and Box test (Fisher's F asymptotic approximation)

Chi-square asymptotic approximation		Fisher's F asymptotic approximation	
-2Log(M)	36.565	-2Log(M)	36.565
Chi-square (Observed value)	25.383	F (Observed value)	2.445
Chi-square (Critical value)	18.307	F (Critical value)	1.855
Degree of freedom	10	Degree of freedom 1	10
p-value	0.005	Degree of freedom 2	392
alpha	0.05	p-value	0.008
		alpha	0.05

Table 9 illustrates the distance between classes is defined by Mahalanobis distance taking into account the structure of covariance.

Table 9: Mahalanobis distance

class	rancid beef	healthy beef
rancid beef	0	10.274
healthy beef	10.274	0

4.5 Classes Mean Vector Un-equality Test

Wilks' Lambda test (Rao approximation) was used to test the assumption of equality between the two classes (healthy or rancid) for beef. When there are only two classes the Wilks' Lambda test is similar to the Fisher test. Wilks' Lambda test increases accuracy when there are more than two classes. Since the computed P-value is less than the alpha significance level = 0.05, the null hypothesis H0 is rejected, and the alternative hypothesis Ha is accepted, as depicted in Table 10.

Table 10: Wilks' Lambda test (Rao's approximation)

Lambda	0.322
F (Observed value)	9.983
F (Critical value)	2.895
Degree of freedom 1	4
Degree of freedom 2	19
p-value	0.000
alpha	0.05

4.6 Eigenvalue Calculation; Significance Test Between Classes

Table 11 indicates that the matrix affects the vector, in terms of the magnitude and direction of the vector. The matrix affects some vectors in changing their magnitude only or in their orientation only. Also, the matrix affects the eigenvector, when multiplied by a specified parameter. The eigenvector is positive, when there is no change in its orientation. However, the eigenvector is negative, when a change in its direction and magnitude occurs. This parameter is the eigenvalue of the eigenvector.

Table 11: The associated eigenvalues and the corresponding percentages of discrimination and cumulative

Item	value
Eigenvalue	2.102
Discrimination, %	100.000
Cumulative, %	100.000

Table 12 illustrates the Bartlett's test on significance of eigenvalues: It also presents the significance test for eigenvalues through the computed P-value that is calculated using the Chi-square test. Bartlett's test is based on testing the null hypothesis H0 that supposes all eigenvalues are equal to zero. Since the computed P-value is less than the alpha significance level = 0.05, one must reject the null hypothesis H0, and accept the alternative hypothesis, Ha.

Table 12: Bartlett's test for eigenvalue significance

Item	value
Eigenvalue	2.102
Bartlett's statistic	22.638
p-value	0.000

4.7 Classifier Performance Evaluation Test

4.7.1 Correlations Relation of Variables

Table 13 indicates the correlations between variables, which represent in the color frequencies (Red, Green, and Blue) and light reflection. It was found that the high correlation factor between the red frequencies, it was 0.972.

Table 13: Variables correlations

Variable	Correlation factor
Reflection	0.845
Blue	0.830
Green	0.879
Red	0.972

4.7.2 Total Classification Variables of LDA

The main objective of LDA is to reach the high classification ratio between two classes (healthy or rancid), through the covariance matrix. If they are equal, the classification is linear, and if the covariance matrix is not equal, the classification is quadratic. Table 14 indicates the total coefficient of classification using a model LDA for the calibration set was of 100% and the validation set was of 91.67%.

Table 14: LDA model for classification samples during storage days of beef

Calibration set					Validation set			
From/to	rancid	healthy	Total	%correct	rancid	healthy	Total	%correct
rancid	4	0	4	100.00	6	0	6	100.00
healthy	0	12	12	100.00	2	16	18	88.89
Total	4	12	16	100.00	8	16	24	91.67

4.7.3 Dimensional Reduction by PCA

The main objective of PCA is to obtain a smaller set of linear grouping by summarizing a set of variables, and reducing dimensions in order to, speed up the data processing process. Table 15 demonstrates the correlation coefficient between variables that represent the color frequencies and the reflection spectra of the samples (Red, Green, Blue, and Reflection), respectively.

Table 15: Correlation matrix (Pearson (n))

Variable	Reflection	Blue	Green	Red
Reflection	1	0.927	0.921	0.865
Blue	0.927	1	0.961	0.919
Green	0.921	0.961	1	0.923
Red	0.865	0.919	0.923	1

Values listed in Table 15, are different from 0 with a significance level alpha=0.05. The next Table 16 and the corresponding chart, Figure 5, are related to a mathematical object, the eigenvalues, which reflect the quality of the projection from the N-dimensional initial table to a lower number of dimensions.

Table 16: Eigenvalues

Item	F1	F2	F3	F4
Eigenvalue	3.759	0.135	0.067	0.038
Variability, %	93.978	3.376	1.684	0.962
Cumulative, %	93.978	97.354	99.038	100.000

Figure 5 shows the correlation circle (below on axes F1 and F2) among the discrimination variables of reflectance spectrum and frequencies of RGB color sensor. The new spatial dimensions can represent 97.35% of the whole discrimination of beef samples. The discrimination variables on the correlation circle are most related to the dimension of F1 of 93.98%. A PCA bi-plot shows the values of the variables (points) and their direction of the variables (vectors). The angle values between vectors also indicate the extent to which variables are related to each other: acute angle indicates positive correlation, large angle indicates negative correlation, and 90-degree angle indicates no correlation between two variables. A scree plot chart shows the amount of variance that each major component of the data captures. Figure 6 shows the low angle between the blue and green frequency, so the correlation between them was positive and strong. The arrows contain the information on loadings or represent the vectors of the variables. The length of the variables vector illustrates how well the variables are represented by the graph with a perfect fit. The length of the stock is directly proportional to the variance of the data, so the shortest arrows are the frequency of the blue and green colors, which indicates a decrease in the variance and an increase in the data correlation.

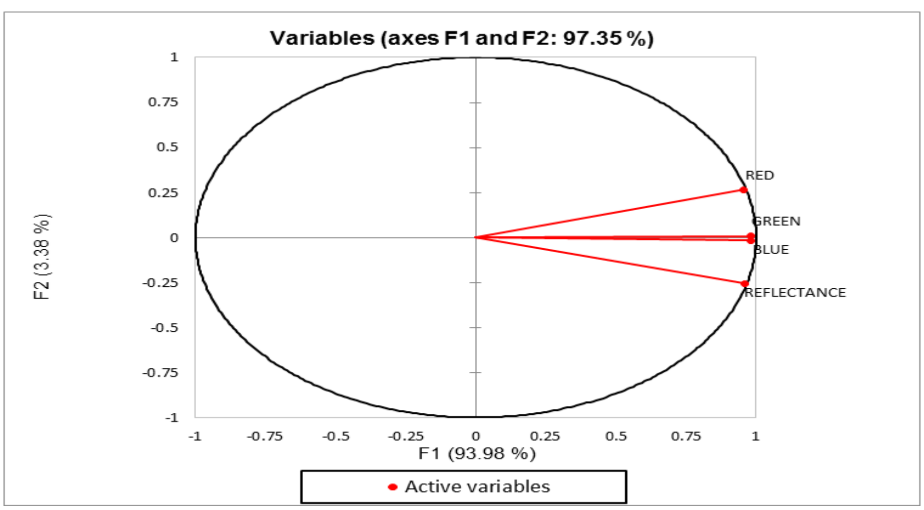

Fig. 5: Correlation circle of discrimination variables

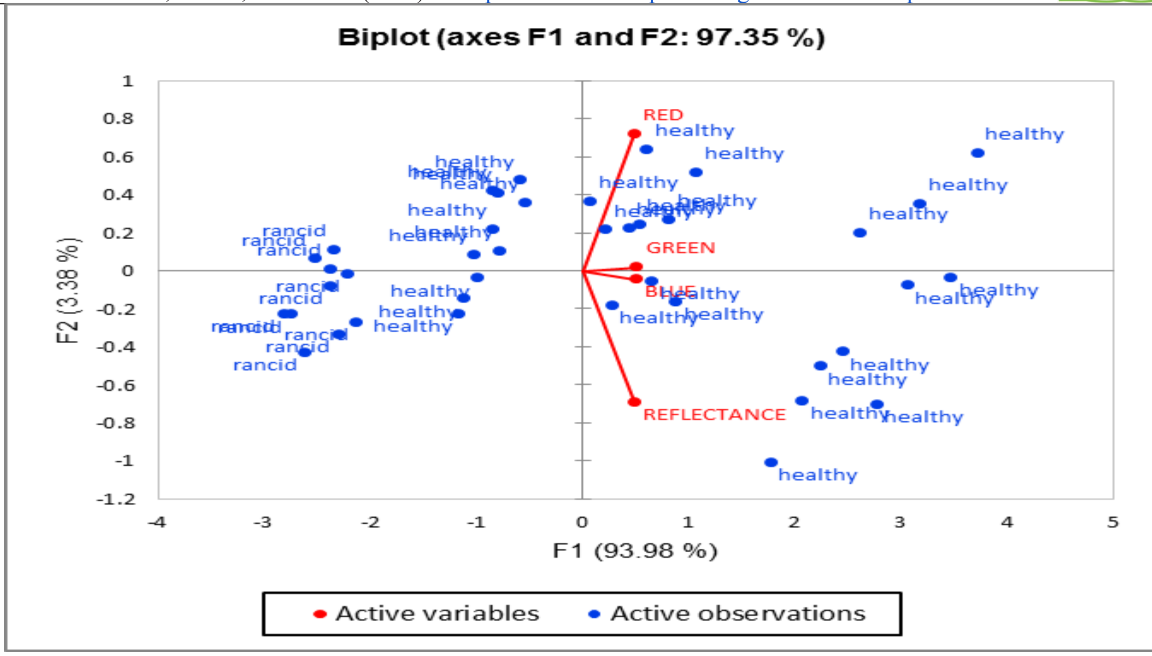

Fig. 6: Biplots representation of observations (healthy and rancid beef) and variables (Red, Green, Blue and Reflectance) on the new dimensional space

Table 17 illustrates Values in F1 match for each variable to the factor for which the squared cosine is the largest.

Table 17: Squared cosines of the variables at the new dimensional space of F1, F2, F3, F4

Variables	F1	F2	F3	F4
Reflection	**0.917**	0.065	0.019	0.000
Blue	**0.965**	0.000	0.015	0.020
Green	**0.964**	0.000	0.017	0.019
Red	**0.914**	0.070	0.016	0.000

5 Conclusions

The quality of beef samples was classified into two categories, healthy and rancid, using two models of Support Vector Machine and Linear Discrimination Analysis. The total classification percentage for Support Vector Machine model for the calibration set was of 95.83% and the validation set was of 93.75%. The total coefficient of classification for Linear Discrimination Analysis model for the calibration set was of 100% and the validation set was of 91.67%. To reduce data representation dimensions, Principal Component Analysis was used and the score plot percentage of (F1 & F2) of forty samples were of 93.98% and 3.38%, respectively. Therefore, the quality of beef can be predicted by Support Vector Machine was the best classifier model that represents 95.75% from the whole data.

Conflict of interest

The authors declare that there is no conflict regarding the publication of this paper.

References

[1] Hu, Z. and Sun, D.-W. CFD simulation of heat and moisture transfer for predicting cooling rate and weight loss of cooked ham during air-blast chilling process. Journal of Food Engineering, 46, 3 (2000/11/01/ 2000), 189-197.

[2] McDonald, K. and Sun, D.-W. The formation of pores and their effects in a cooked beef product on the efficiency of vacuum cooling. Journal of Food Engineering, 47, 3 (2001/02/01/ 2001), 175-183.

[3] Kiani, H., Sun, D. W., Delgado, A. and Zhang, Z. Investigation of the effect of power ultrasound on the nucleation of water during freezing of agar gel samples in tubing vials. Ultrasonics sonochemistry, 19, 3 (May 2012), 576-581.

[4] Ma, J., Pu, H., Sun, D.-W., Gao, W., Qu, J.-H. and Ma, K.-Y. Application of Vis–NIR hyperspectral imaging in classification between fresh and frozen-thawed pork Longissimus Dorsi muscles. International Journal of Refrigeration, 50(2015/02/01/ 2015), 10-18.

[5] Xie, A., Sun, D. W., Xu, Z. and Zhu, Z. Rapid detection of frozen pork quality without thawing by Vis-NIR hyperspectral imaging technique. Talanta, 139(Jul 1 2015), 208-215.

[6] Xie, A., Sun, D.-W., Zhu, Z. and Pu, H. Nondestructive Measurements of Freezing Parameters of Frozen Porcine Meat by NIR Hyperspectral Imaging. Food and Bioprocess Technology, 9, 9 (2016/09/01 2016), 1444-1454.

[7] Qu, J.-H., Sun, D.-W., Cheng, J.-H. and Pu, H. Mapping moisture contents in grass carp (Ctenopharyngodon idella) slices under different freeze drying periods by Vis-NIR hyperspectral imaging. LWT, 75(2017/01/01/ 2017), 529-536.

[8] Cheng, J.-H., Sun, D.-W. and Pu, H. Combining the genetic algorithm and successive projection algorithm for the selection of feature wavelengths to evaluate exudative characteristics in frozen–thawed fish muscle. Food chemistry, 197(2016/04/15/ 2016), 855-863.

[9] Cheng, L., Sun, D. W., Zhu, Z. and Zhang, Z. Emerging techniques for assisting and accelerating food freezing processes: A review of recent research progresses. Critical reviews in food science and nutrition, 57, 4 (Mar 4 2017), 769-781.

[10] Cheng, W., Sun, D.-W., Pu, H. and Wei, Q. Characterization of myofibrils cold structural deformation degrees of frozen pork using hyperspectral imaging coupled with spectral angle mapping algorithm. Food chemistry, 239(2018/01/15/ 2018), 1001-1008.

[11] Pu, Y.-Y. and Sun, D.-W. Prediction of moisture content uniformity of microwave-vacuum dried mangoes as affected by different shapes using NIR hyperspectral imaging. Innovative Food Science & Emerging Technologies, 33(2016/02/01/ 2016), 348-356.

[12] Pu, Y.-Y. and Sun, D.-W. Combined hot-air and microwave-vacuum drying for improving drying uniformity of mango slices based on hyperspectral imaging visualisation of moisture content distribution. Biosystems Engineering, 156(2017/04/01/ 2017), 108-119.

[13] Ma, J., Sun, D.-W., Qu, J.-H. and Pu, H. Prediction of textural changes in grass carp fillets as affected by vacuum freeze drying using hyperspectral imaging based on integrated group wavelengths. LWT - Food Science and Technology, 82(2017/09/01/ 2017), 377-385.

[14] Sun, D.-W. and Brosnan, T. Pizza quality evaluation using computer vision—Part 2: Pizza topping analysis. Journal of Food Engineering, 57, 1 (2003/03/01/ 2003), 91-95.

[15] Du, C. J. and Sun, D. W. Pizza sauce spread classification using colour vision and support vector machines. Journal of food engineering., 66, 2 (2005/01// 2005), 137-145.

[16] Jackman, P., Sun, D.-W., Du, C.-J. and Allen, P. Prediction of beef eating qualities from colour, marbling and wavelet surface texture features using homogenous carcass treatment. Pattern Recognition, 42, 5 (2009/05/01/ 2009), 751-763.

[17] Jackman, P., Sun, D.-W. and Allen, P. Recent advances in the use of computer vision technology in the quality assessment of fresh meats. Trends in Food Science & Technology, 22, 4 (2011/04/01/ 2011), 185-197.

[18] Vidal, A., Talens, P., Prats-Montalbán, J. M., Cubero, S., Albert, F. and Blasco, J. In-Line Estimation of the Standard Colour Index of Citrus Fruits Using a Computer Vision System Developed For a Mobile Platform. Food and Bioprocess Technology, 6, 12 (2013/12/01 2013), 3412-3419.

[19] Xu, J.-L., Riccioli, C. and Sun, D.-W. Comparison of hyperspectral imaging and computer vision for automatic differentiation of organically and conventionally farmed salmon. Journal of Food Engineering, 196(2017/03/01/ 2017), 170-182.

[20] Xu, J.-L. and Sun, D.-W. Identification of freezer burn on frozen salmon surface using hyperspectral imaging and computer vision combined with machine learning algorithm. International Journal of Refrigeration, 74(2017/02/01/ 2017), 151-164.

[21] Shao, Y., Zhao, C., Bao, Y. and He, Y. Quantification of Nitrogen Status in Rice by Least Squares Support Vector Machines and Reflectance Spectroscopy. Food and Bioprocess Technology, 5, 1 (2012/01/01 2012), 100-107.

[22] Wu, D., Nie, P., He, Y. and Bao, Y. Determination of Calcium Content in Powdered Milk Using Near and Mid-Infrared Spectroscopy with Variable Selection and Chemometrics. Food and Bioprocess Technology, 5, 4 (2012/05/01 2012), 1402-1410.

[23] Ye, M., Yue, T., Yuan, Y. and Li, Z. Application of FT-NIR Spectroscopy to Apple Wine for Rapid Simultaneous

Determination of Soluble Solids Content, pH, Total Acidity, and Total Ester Content. Food and Bioprocess Technology, 7, 10 (2014/10/01 2014), 3055-3062.

[24] Zhang, H., Wang, J., Ye, S. and Chang, M. Application of Electronic Nose and Statistical Analysis to Predict Quality Indices of Peach. Food and Bioprocess Technology, 5, 1 (2012/01/01 2012), 65-72.

[25] Hong, X. and Wang, J. Use of Electronic Nose and Tongue to Track Freshness of Cherry Tomatoes Squeezed for Juice Consumption: Comparison of Different Sensor Fusion Approaches. Food and Bioprocess Technology, 8, 1 (2015/01/01 2015), 158-170.

[26] Huang, L., Liu, H., Zhang, B. and Wu, D. Application of Electronic Nose with Multivariate Analysis and Sensor Selection for Botanical Origin Identification and Quality Determination of Honey. Food and Bioprocess Technology, 8, 2 (2015/02/01 2015), 359-370.

[27] Dutta, S., Bhattacharjee, P. and Bhattacharyya, N. Assessment of Shelf Lives of Black Pepper and Small Cardamom Cookies by Metal Oxide-Based Electronic Nose Using Spoilage Index. Food and Bioprocess Technology, 10, 11 (2017/11/01 2017), 2023-2033.

[28] ElMasry, G., Sun, D.-W. and Allen, P. Chemical-free assessment and mapping of major constituents in beef using hyperspectral imaging. Journal of Food Engineering, 117, 2 (2013/07/01/ 2013), 235-246.

[29] Xiong, Z., Sun, D.-W., Pu, H., Xie, A., Han, Z. and Luo, M. Non-destructive prediction of thiobarbituricacid reactive substances (TBARS) value for freshness evaluation of chicken meat using hyperspectral imaging. Food chemistry, 179(2015/07/15/ 2015), 175-181.

[30] Pu, H., Sun, D.-W., Ma, J. and Cheng, J.-H. Classification of fresh and frozen-thawed pork muscles using visible and near infrared hyperspectral imaging and textural analysis. Meat Science, 99(2015/01/01/ 2015), 81-88.

[31] Pu, H., Xie, A., Sun, D.-W., Kamruzzaman, M. and Ma, J. Application of Wavelet Analysis to Spectral Data for Categorization of Lamb Muscles. Food and Bioprocess Technology, 8, 1 (2015/01/01 2015), 1-16.

[32] Cheng, J.-H. and Sun, D.-W. Rapid and non-invasive detection of fish microbial spoilage by visible and near infrared hyperspectral imaging and multivariate analysis. LWT - Food Science and Technology, 62, 2 (2015/07/01/ 2015), 1060-1068.

[33] Cheng, J.-H., Sun, D.-W., Pu, H. and Zhu, Z. Development of hyperspectral imaging coupled with chemometric analysis to monitor K value for evaluation of chemical spoilage in fish fillets. Food chemistry, 185(2015/10/15/ 2015), 245-253.

[34] Cheng, J.-H., Sun, D.-W., Pu, H.-B., Wang, Q.-J. and Chen, Y.-N. Suitability of hyperspectral imaging for rapid evaluation of thiobarbituric acid (TBA) value in grass carp (Ctenopharyngodon idella) fillet. Food chemistry, 171(2015/03/15/ 2015), 258-265.

[35] Cheng, J.-H., Sun, D.-W., Qu, J.-H., Pu, H.-B., Zhang, X.-C., Song, Z., Chen, X. and Zhang, H. Developing a multispectral imaging for simultaneous prediction of freshness indicators during chemical spoilage of grass carp fish fillet. Journal of Food Engineering, 182(2016/08/01/ 2016), 9-17.

[36] Ma, J., Sun, D. W. and Pu, H. Spectral absorption index in hyperspectral image analysis for predicting moisture contents in pork longissimus dorsi muscles. Food chemistry, 197, Pt A (Apr 15 2016), 848-854.

[37] Xu, J.-L., Riccioli, C. and Sun, D.-W. Development of an alternative technique for rapid and accurate determination of fish caloric density based on hyperspectral imaging. Journal of Food Engineering, 190(2016/12/01/ 2016), 185-194.

[38] Dai, Q., Cheng, J.-H., Sun, D.-W., Zhu, Z. and Pu, H. Prediction of total volatile basic nitrogen contents using wavelet features from visible/near-infrared hyperspectral images of prawn (Metapenaeus ensis). Food chemistry, 197(2016/04/15/ 2016), 257-265.

[39] Ravikanth, L., Jayas, D. S., White, N. D. G., Fields, P. G. and Sun, D.-W. Extraction of Spectral Information from Hyperspectral Data and Application of Hyperspectral Imaging for Food and Agricultural Products. Food and Bioprocess Technology, 10, 1 (2017/01/01 2017), 1-33.

[40] Li, J.-L., Sun, D.-W., Pu, H. and Jayas, D. S. Determination of trace thiophanate-methyl and its metabolite carbendazim with teratogenic risk in red bell pepper (Capsicumannuum L.) by surface-enhanced Raman imaging technique. Food chemistry, 218(2017/03/01/ 2017), 543-552.

[41] Goyache, F., Bahamonde, A., Alonso, J., Lopez, S., del Coz, J. J., Quevedo, J. R., Ranilla, J., Luaces, O., Alvarez,

I., Royo, L. J. and Diez, J. The usefulness of artificial intelligence techniques to assess subjective quality of products in the food industry. Trends in Food Science & Technology, 12, 10 (2001/10/01/ 2001), 370-381.

[42] Jia, W., Li, Y., Qu, R., Baranowski, T., Burke, L. E., Zhang, H., Bai, Y., Mancino, J. M., Xu, G., Mao, Z. H. and Sun, M. Automatic food detection in egocentric images using artificial intelligence technology. Public health nutrition, 22, 7 (May 2019), 1168-1179.

[43] Camaréna, S. Artificial intelligence in the design of the transitions to sustainable food systems. Journal of Cleaner Production, 271(2020/10/20/ 2020), 122574.

[44] Bourguet, J.-R., Thomopoulos, R., Mugnier, M.-L. and Abécassis, J. An artificial intelligence-based approach to deal with argumentation applied to food quality in a public health policy. Expert Systems with Applications, 40, 11 (2013/09/01/ 2013), 4539-4546.

[45] Sun, Q., Zhang, M. and Mujumdar, A. S. Recent developments of artificial intelligence in drying of fresh food: A review. Critical reviews in food science and nutrition, 59, 14 (2019/08/06 2019), 2258-2275.

[46] Di Vaio, A., Boccia, F., Landriani, L. and Palladino, R. Artificial Intelligence in the Agri-Food System: Rethinking Sustainable Business Models in the COVID-19 Scenario. Sustainability, 12(06/14 2020), 4851.

[47] Wuest, T., Weimer, D., Irgens, C. and Thoben, K.-D. Machine learning in manufacturing: advantages, challenges, and applications. Production & Manufacturing Research, 4, 1 (2016/01/01 2016), 23-45.

[48] Ge, Z., Song, Z., Ding, S. X. and Huang, B. Data Mining and Analytics in the Process Industry: The Role of Machine Learning. IEEE Access, 52017), 20590-20616.

[49] Fujimoto, Y., Murakami, S., Kaneko, N., Fuchikami, H., Hattori, T. and Hayashi, Y. Machine Learning Approach for Graphical Model-Based Analysis of Energy-Aware Growth Control in Plant Factories. IEEE Access, 72019), 32183-32196.

[50] Balasubramanya, N. Experimental Study on Light Weight Concrete using Leca and Cinder as Coarse Aggregates. International Journal of Engineering research and Technology, Vol. 4(07/01 2015), 52-54.

[51] Mizushima, A. and Lu, R. An image segmentation method for apple sorting and grading using support vector machine and Otsu’s method. Computers and Electronics in Agriculture, 94(2013/06/01/ 2013), 29-37.

[52] Ebrahimi, M. A., Khoshtaghaza, M. H., Minaei, S. and Jamshidi, B. Vision-based pest detection based on SVM classification method. Comput. Electron. Agric., 137, C 2017), 52–58.

[53] Azarmdel, H., Jahanbakhshi, A., Mohtasebi, S. S. and Muñoz, A. R. Evaluation of image processing technique as an expert system in mulberry fruit grading based on ripeness level using artificial neural networks (ANNs) and support vector machine (SVM). Postharvest Biology and Technology, 166(2020/08/01/ 2020), 111201.

[54] Wang, X.-Y., Wang, T. and Bu, J. Color image segmentation using pixel wise support vector machine classification. Pattern Recognition, 44, 4 (2011/04/01/ 2011), 777-787.

[55] Kelly, S., Heaton, K. and Hoogewerff, J. Tracing the geographical origin of food: The application of multi-element and multi-isotope analysis. Trends in Food Science & Technology, 16, 12 (2005/12/01/ 2005), 555-567.

[56] Li, X., Yang, S., Fan, R., Yu, X. and Chen, D. Discrimination of soft tissues using laser-induced breakdown spectroscopy in combination with k nearest neighbors (kNN) and support vector machine (SVM) classifiers. Optics & Laser Technology, 102(2018/06/01/ 2018), 233-239.

[57] Minija, S. J. and Emmanuel, W. R. S. Food image classification using sphere shaped — Support vector machine. 2017 International Conference on Inventive Computing and Informatics (ICICI)2017), 109-113.

[58] Marchesan, G., Muraro, M. R., Cardoso, G., Mariotto, L. and da Silva, C. D. L. Method for distributed generation anti-islanding protection based on singular value decomposition and linear discrimination analysis. Electric Power Systems Research, 130(2016/01/01/ 2016), 124-131.

[59] Yu, H., Wang, Y. and Wang, J. Identification of tea storage times by linear discrimination analysis and back-propagation neural network techniques based on the eigenvalues of principal components analysis of e-nose sensor signals. Sensors (Basel, Switzerland), 9, 10 2009), 8073-8082.

[60] Kašpárek, T., Thomaz, C. E., Sato, J. R., Schwarz, D., Janousová, E., Mareček, R., Přikryl, R., Vaníček, J., Fujita, A. and Češková, E. Maximum-uncertainty linear discrimination analysis of first-episode schizophrenia subjects. Psychiatry Research: Neuroimaging, 1912011), 174-181.

[61] Huang, S., Li, J., Ye, J., Chen, K., Wu, T., Fleisher, A. and Reiman, E. Identifying Alzheimer's disease-related brain regions from multi-modality neuroimaging data using sparse composite linear discrimination analysis. In Proceedings of the Proceedings of the 24th International Conference on Neural Information Processing Systems (Granada, Spain, 2011). Curran Associates Inc., [insert City of Publication],[insert 2011 of Publication].

[62] D'Archivio, A. A. and Maggi, M. A. Geographical identification of saffron (Crocus sativus L.) by linear discriminant analysis applied to the UV–visible spectra of aqueous extracts. Food chemistry, 219(2017/03/15/ 2017), 408-413.

[63] Esteki, M., Shahsavari, Z. and Simal-Gandara, J. Use of spectroscopic methods in combination with linear discriminant analysis for authentication of food products. Food Control, 91(2018/09/01/ 2018), 100-112.

[64] De Luca, M., Terouzi, W., Kzaiber, F., Ioele, G., Oussama, A. and Ragno, G. Classification of moroccan olive cultivars by linear discriminant analysis applied to ATR–FTIR spectra of endocarps. International Journal of Food Science & Technology, 47, 6 2012), 1286-1292.

[65] Rezzi, S., Giani, I., Héberger, K., Axelson, D. E., Moretti, V. M., Reniero, F. and Guillou, C. Classification of Gilthead Sea Bream (Sparus aurata) from 1H NMR Lipid Profiling Combined with Principal Component and Linear Discriminant Analysis. Journal of Agricultural and Food Chemistry, 55, 24 (2007/11/01 2007), 9963-9968.

[66] Brito, A. L. B., Brito, L. R., Honorato, F. A., Pontes, M. J. C. and Pontes, L. F. B. L. Classification of cereal bars using near infrared spectroscopy and linear discriminant analysis. Food Research International, 51, 2 (2013/05/01/ 2013), 924-928.

[67] Bryant, F. B. and Yarnold, P. R. Principal-components analysis and exploratory and confirmatory factor analysis. American Psychological Association, City, 1995.

[68] Reid, M. K. and Spencer, K. L. Use of principal components analysis (PCA) on estuarine sediment datasets: The effect of data pre-treatment. Environmental Pollution, 157, 8 (2009/08/01/ 2009), 2275-2281.

[69] He, Y., Li, X. and Deng, X. Discrimination of varieties of tea using near infrared spectroscopy by principal component analysis and BP model. Journal of Food Engineering, 79, 4 (2007/04/01/ 2007), 1238-1242.

[70] Guillén-Casla, V., Rosales-Conrado, N., León-González, M. E., Pérez-Arribas, L. V. and Polo-Díez, L. M. Principal component analysis (PCA) and multiple linear regression (MLR) statistical tools to evaluate the effect of E-beam irradiation on ready-to-eat food. Journal of Food Composition and Analysis, 24, 3 (2011/05/01/ 2011), 456-464.

[71] Ghosh, D. and Chattopadhyay, P. Application of principal component analysis (PCA) as a sensory assessment tool for fermented food products. Journal of Food Science and Technology, 49, 3 (2012/06/01 2012), 328-334.

[72] Johnson, G. and Jennings, R. LabVIEW Graphical Programming. Mcgraw-hill, 2006.

[73] Ray, S. Understanding Support Vector Machine(SVM) algorithm from examples (along with code). City, 2017.

[74] Wikipedia Linear discriminant analysis. wikipedia, City, 2020.

[75] Wikipedia Linear discriminant analysis: Revision history. City, 2020.

[76] Bartholomew, D. J. Analysis and Interpretation of Multivariate Data. Elsevier, City, 2010.